

Optical Properties of Polymer-Based Photonic Nanocomposite Materials

Michael R. Bockstaller and Edwin L. Thomas*

Department of Materials Science and Engineering and Institute of Soldier Nanotechnologies,
Massachusetts Institute of Technology, 77 Massachusetts Avenue, Cambridge, Massachusetts 02139

Received: May 9, 2003

Designing metallodielectric nanocomposite materials for photonic applications implies the ability to reliably model and predict the effect of metallic inclusions on the optical properties of a microstructured composite material. We present a detailed analysis of the optical properties of block copolymer based, multilayered metallodielectric Bragg reflectors and discuss the implications of nanosize-specific effects on the design of composite materials for photonic applications. A series of lamellar poly(styrene-*b*-ethylene/propylene) copolymer thin films with varying filling fraction of gold nanocrystals preferentially but randomly distributed within the poly(styrene) domains have been studied by reflectometry. The reflective properties are compared to model calculations based on effective medium concepts taking into account confinement effects on the dielectric function of the nanocrystals. The particle size causes strong alterations in the dielectric function of the metal inclusions that have relevance for the attainable dielectric contrast within periodic nanocomposites.

Introduction

Photonic crystals are microstructured materials in which the dielectric function is periodically modulated in space; a simple example is a 1D multilayer stack, the so-called Bragg reflector, consisting of two alternating materials differing in their index of refraction. Multiple interference between the waves scattered from each unit cell of the structure may result in a “photonic band gap”, a forbidden frequency range, in which light cannot propagate through the structure.^{1,2} Despite their potential, for example, in the design of novel optoelectronic devices, the realization of photonic crystals for optical or near-infrared frequencies is still a major technological challenge requiring new approaches for refractive index engineering.^{3,4} Self-assembly of block copolymers provides an elegant bottom-up approach for fabricating photonic materials for the optical region because they organize into periodic 1D (lamellar), 2D (cylindrical), or 3D (cubic) morphologies with characteristic length scales that can be tailored to be on the order of the wavelength of light.^{5,6} Self-assembly becomes particularly versatile when inorganic nanoparticles are added to the polymer material thereby combining the advantageous processing and mechanical properties of the polymer matrix with the unique optical and magnetic properties of nanoparticles.^{7,8} Recently, we demonstrated that by preferential sequestering of polymer-coated gold nanocrystals within microphase-separated diblock copolymers, metallodielectric photonic materials can be obtained that exhibit high rejection levels for incident light.⁹ Technological relevance of these materials is intimately linked to a fundamental understanding of the relationship between the optical properties of the nanocomposite and the structural characteristics at the nano- and mesoscale level so as to afford reliable prediction of the photonic properties to tailor the materials for various applications. Assuming the inclusions to be small enough to neglect other than dipolar excitations as response to an incident electromagnetic field (quasi-static approximation), Lorentz local field relations can be used to determine the effective dielectric

function, ϵ_{eff} , of the composite material.¹⁰ Effective medium theory (EMT) has been successful in describing the optical properties of homogeneous sol–gels containing a variety of spherically shaped metal nanocrystals.^{11,12}

The aim of this contribution is to demonstrate the relevance of size-specific alterations of the optical properties of the nanocrystals to the photonic properties of mesoscopically ordered nanocomposite materials. We present a detailed study of the optical properties of self-assembled lamellar block copolymer/gold nanocrystal composites, in which the nanocrystals are preferentially sequestered within one polymer domain. For this purpose, the use of ex situ synthesized polymer-grafted nanocrystals is advantageous for two reasons: (1) it provides an effective means to avoid aggregation when the particles are dispersed within polymer matrixes, even at high filling fractions, resulting in well-defined morphologies and (2) it decouples the particle synthesis from microstructure formation and is hence applicable to a broad range of material compositions. The resulting nanoparticle-filled materials represent model systems to study the optical properties of microstructured composite materials that capitalize not only on the periodic morphology of the polymer matrix but also on the particular optical properties of the dispersed component.

The outline of the paper is as follows: the first part comprises a structural characterization of the material samples. The preferential sequestering of the surface-tailored nanocrystals within lamellar block copolymer morphology, as well as the effect of particle sequestering on the sample reflectivity, is presented. A study of the optical properties of homopolymer/nanocrystal composites that represent a simple model system to study the effect of nanocrystal content on the optical properties of the composite material is the focus of the second part. The results are compared to effective medium calculations using Maxwell–Garnett theory, and the lack of agreement with calculations based on bulk values for the optical constants of gold is pointed out. In the third part of the paper, the results obtained for the homopolymer/nanocrystal composite are used to rationalize the observed photonic properties of the block

* To whom correspondence should be addressed. E-mail: elt@mit.edu.

copolymer/nanocrystal composites. The implications on the design of microstructured composite materials for photonic applications are also discussed.

Materials and Methods

All chemicals were purchased from Aldrich. Ethylenesulfide was distilled prior to use. The poly(styrene) (PS) homopolymer $M_w = 30$ kg/mol was purchased from Polysciences. The synthesis of the near-symmetric poly(styrene-*b*-ethylene/propylene) (PS-PEP) $M_w = 400$ – 400 kg/mol block copolymer having an index of polydispersity (PDI) of 1.04 has been described elsewhere.⁵ Thiol-terminated oligo(styrene) ligands were synthesized by anionic polymerization at 25 °C in benzene. Adding ethylenesulfide to the reaction mixture stopped the reaction. The thiol-terminated oligo(styrene) ligands were characterized by size exclusion chromatography (SEC) using poly(styrene) calibration yielding a molecular weight of $M_n = 980$ g/mol corresponding a degree of polymerization of $P \approx 9$ and PDI = 1.08. The product was purified before further reaction by precipitation out of benzene solution by the addition of methanol.

The synthetic procedure employed to grow the oligo(styrene)-coated gold nanocrystals was according to the one described in the literature,¹³ using the thiol-terminated oligo(styrene) as a ligand. The reaction product was precipitated in methanol/ethanol (1:1), and the excess ligand was removed by washing with ethanol/THF (5:1).

The metallodielectric nanocomposites were prepared by controlled solvent evaporation of a toluene solution of homopolymer or block copolymer (2 mL, 5%) after adding gold nanocrystals (0.5 mL, 1–15% in toluene). After evaporation of the solvent, the films were kept 72 h in oversaturated solvent atmosphere at 60 °C (solvent annealing) and thereafter dried in a vacuum for 12 h. For reflectance measurements, thin films were prepared by the following procedure: 0.15 mL of a 1% polymer solution in toluene with appropriate fraction of gold nanocrystals was cast on a silica cover slip (18 mm diameter) that was previously coated with surfactant (Victawet). The amount of material was calculated to obtain films of about 5 μm thickness. After solvent evaporation (24 h), the samples were solvent-annealed for 48 h and covered with a glass slide and dried in a vacuum for 12 h at 60 °C before measurement.

Transmission electron microscopy was performed using a Joel 2000FX microscope operating at 200 kV. The specimens were prepared by microsectioning using a Reichert-Jung ULTRACUT 4E microtome operating at -120 °C. No stain was used for all micrographs shown.

Absorption measurements were performed using a CARY 5E UV–vis–NIR spectrophotometer equipped with integrating sphere operating in transmission mode.

Subdomain reflectance measurements were performed using a ZEISS Axiophot microscope operating in reflectance mode equipped with a StellarNet EPP2000C spectrophotometer.

The layer spacings of the neat block copolymer were determined using ultrasmall angle scattering as described elsewhere.⁹

Variable angle spectroscopic ellipsometry (VASE) on gold/poly(styrene) films was performed using a Woolham Co. VASE spectroscopic ellipsometer, the data analysis was done using the WVASE32 software package. Measurements were performed from 350 to 700 nm at angles of incidence 65°, 70°, and 75° (close to pseudo-Brewster angle). The samples were prepared by spin casting a 1% solution of PS in toluene containing the appropriate amount of gold nanocrystals (cor-

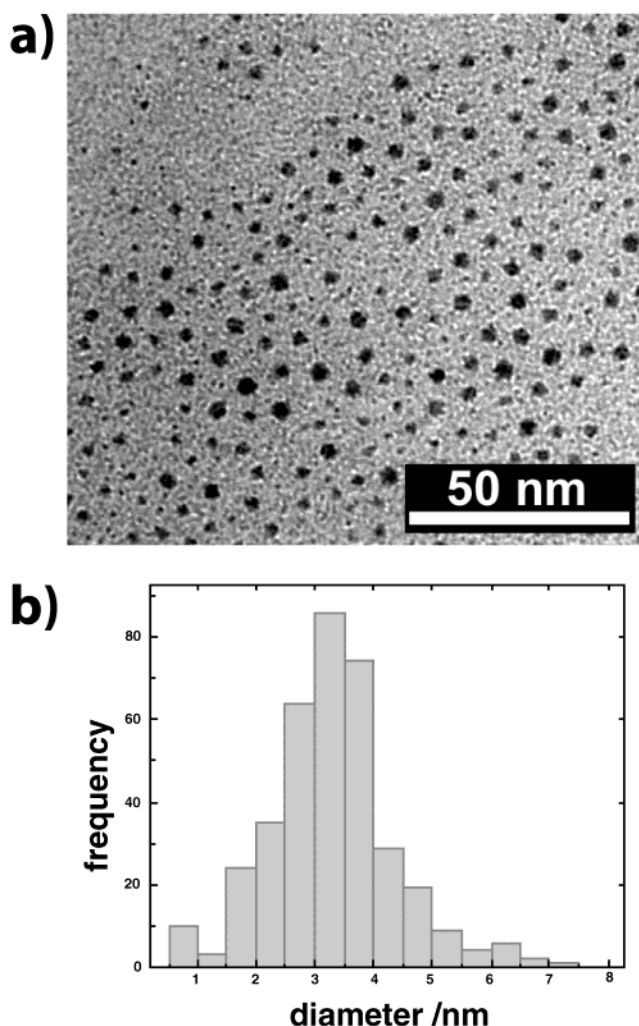


Figure 1. Transmission electron micrograph (a) of the oligo(styrene)-coated gold nanocrystals on a carbon support film. Darker particle contrast arises from Bragg scattering depending on the orientation of the crystal with respect to the incident electron beam. Panel b shows the size distribution revealing mean particle core diameter of $\langle d_{\text{core}} \rangle = 3.5$ nm. Particle sizes were determined by image analysis of electron micrographs using the freeware package SCION IMAGE counting >300 particles.

responding to 0.01–0.12 volume filling fraction of nanocrystals within the polymer) onto a silicon substrate. The spinning conditions were 5000 rpm for 120 s at an acceleration rate of 100 rpm/s at 25 °C. After preparation, all films were dried for 12 h at 60 °C in a vacuum. In all cases, the resultant films were 20–60 nm in thickness.

Profilometry to obtain sample thickness and uniformity was performed using a Tencor P10 profilometer using a scan speed of 20 $\mu\text{m}/\text{s}$ and 6 mg stylus force. The sample preparation was according to the procedure described for the VASE experiments.

Results and Discussion

The synthesis of gold nanocrystals by phase-transfer reaction has been shown to result in uniformly sized particles in which the diameter strongly depends on the gold/thiol molar ratio.^{13,14} We found this synthetic route also to be versatile for synthesizing polymer-coated gold nanocrystals, the only restrictions for the polymer being that it exhibits a mercapto end group as the only reactive site for gold and that it is soluble in toluene. All of the results presented in this paper have been obtained with

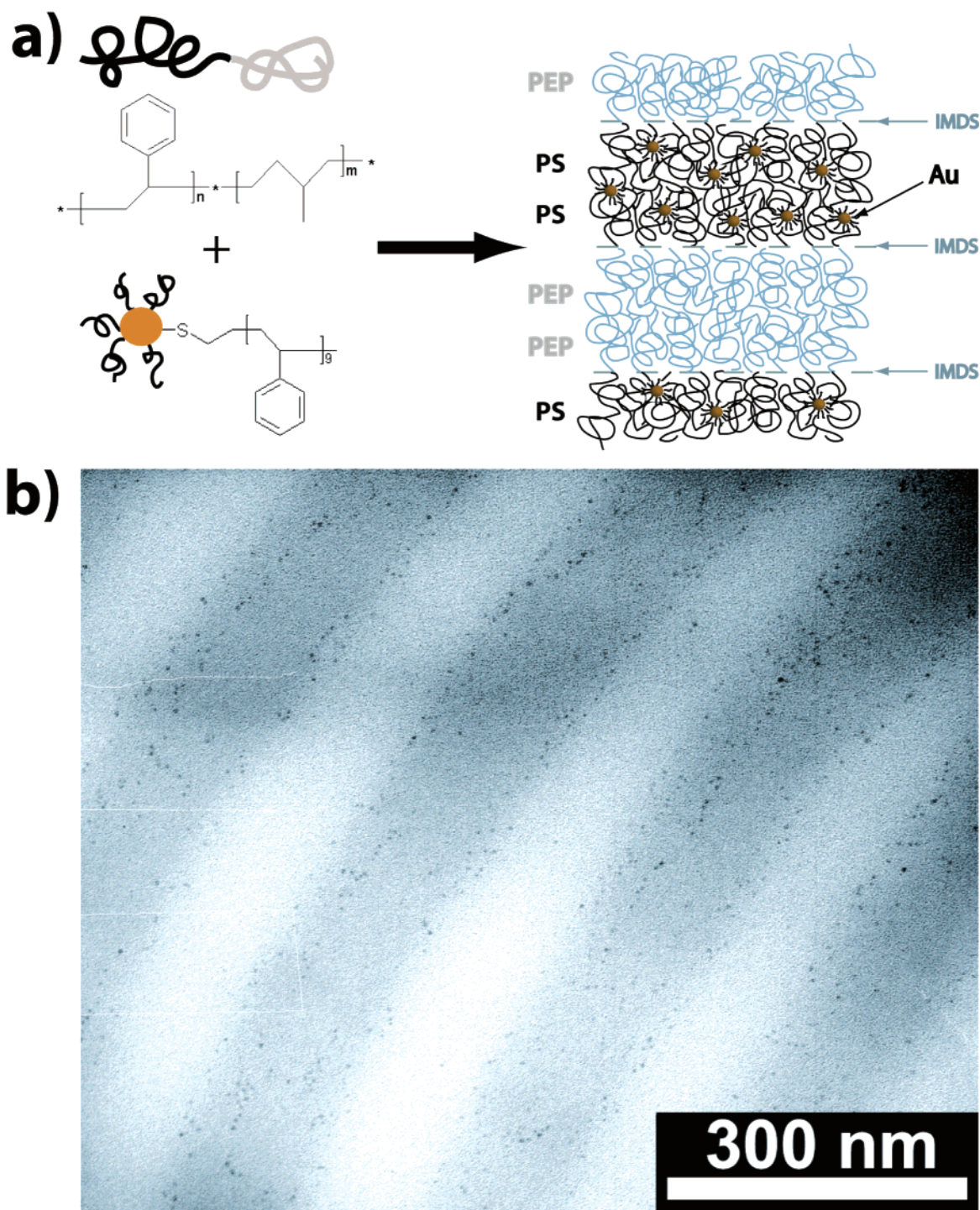


Figure 2. Schematic (a) of the structure formation process that results in the nanocomposite Bragg reflector architecture: oligo(styrene)-coated gold nanocrystals sequester within the poly(styrene) domains of the poly(styrene-*b*-ethylenepropylene) copolymer (PS-PEP) (size proportions are changed for clarity). Degree of polymerization of the PS-PEP block copolymer is $n = 3500$ and $m = 5800$. Panel b shows the underfocused bright field transmission electron micrograph of a section of the unstained PS-PEP/gold nanocrystal composite film after sectioning a fracture surface. The volume filling fraction of the gold nanocrystals within the PS layer is $\phi = 0.06$. The gray areas correspond to the PS layers, and the bright regions to the PEP layers. The gold nanocrystals, visualized by their amplitude (diffraction and mass thickness) contrast appear as dark spots approximately homogeneously distributed within the PS layer.

gold nanocrystals, the core size being $d_{\text{core}} = 3.2 \pm 1.5$ nm, the surface being coated with PS having a molecular weight $M_w = 980$ g/mol. From the nearest-neighbor particle distance that can be determined in particle monolayer films as shown in Figure 1, the dimension of the surfactant layer shell can be estimated to be about $r \approx 1.9$ nm, that is equal to about the radius of gyration of the grafted oligo(styrene) ligands.

The potential of inorganic nanoparticles to tune the optical properties of sol-gel or polymeric matrixes has fueled the interest in nanocomposite materials and has been discussed by several authors.^{15,16} The potential is further increased by the possibility of using block copolymers as material templates and thereby combining the optical properties of the nanoparticles with the optical properties of the block copolymer micro-

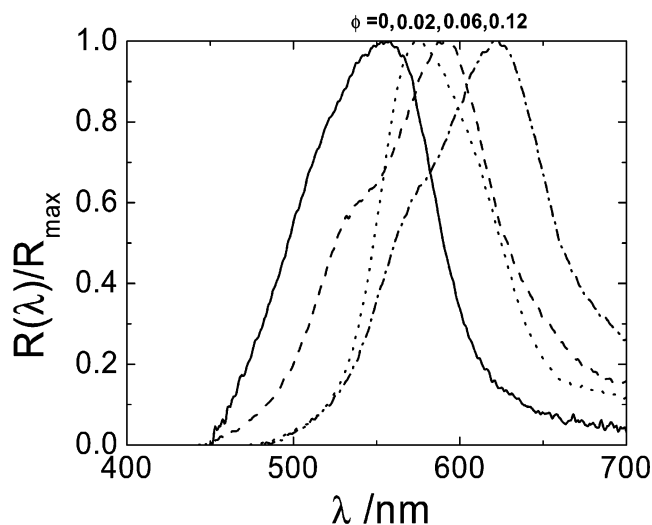


Figure 3. Plot of the normalized reflectivity at normal incidence of thin films (thickness about 5 μm) of the pure block copolymer (—), and the block copolymer/nanocrystal composites with $\phi = 0.02$ (···), 0.06 (---), and 0.12 (— · —).

structure.^{5,9,17–19} As a model system for our studies, we chose a PS–PEP diblock copolymer that microphase separates into a lamellar morphology with layer spacings of the respective domains of $d_{\text{PS}} = 100$ nm and $d_{\text{PEP}} = 80$ nm.⁹ Particles were added to the polymer solution during self-assembly to obtain a lamellar stack of PS–PEP with a gold-crystal filling fraction in the PS domain of $\phi = 0.02, 0.04, 0.06$, and 0.12 . As shown in Figure 2, the PS-coated gold nanocrystals sequester preferentially but homogeneously within the PS domain without a significant tendency for aggregation. Films having a total thickness of about 5 μm were cast onto silica substrates, and the reflective properties were studied from 400 to 800 nm using a compound microscope working in reflectance mode. Normalized reflectance spectra that have been obtained for films of various gold-crystal filling fractions are shown in Figure 3. With increasing gold filling fraction, a red shift in the wavelength of maximum reflectivity can be observed. For example, $\Delta\lambda/\lambda_0 = 0.13$ for the $\phi = 0.12$ sample, λ_0 being the wavelength of maximum reflection of the neat block copolymer. To quantitatively relate the observed wavelength dependence of the peak reflectance to the composition and structural characteristics of the metallodielectric photonic materials is the main interest of the present paper. We focus on the wavelength of maximum reflection rather than on the absolute value of the obtained reflectivity because the latter depends on the exact number of lamellar repeats within the stack—a quantity that is hard to precisely determine for the different films. However, for a lamellar system with lamellar thickness $L = d_1 + d_2$, where L is the total lamellar thickness and d_1 and d_2 are the respective layer spacings, the center frequency of the band gap is intimately linked to the dielectric contrast within the structure and independent of the number of repeats.³ This is demonstrated most readily by assuming the layers to be oriented normal with respect to the incident light resulting in the wavelength of the first-order peak given by $\lambda_{\text{max}} = 2(n_1d_1 + n_2d_2)$, where n_1 and n_2 are the refractive indices of the respective layers.⁵ Therefore, the wavelength corresponding to the maximum reflectivity provides a more robust measure for the change in optical properties of the PS layers due to Au-particle sequestration. Given the preferential localization of the gold nanocrystals within the polystyrene domains and the almost homogeneous particle distribution within the domains as seen in Figure 2, the

optical response of the nanocomposite can be calculated by ascribing to the PS/particle layer an effective dielectric constant, ϵ_{eff} , and calculating the reflectivity using the transfer matrix method.²⁰ However, special care has to be taken regarding the choice of the nanocrystal dielectric function for this approach to account for the experimental values. No agreement could be achieved between the calculated and experimental values for the reflectivity at normal incidence when the dielectric function of the nanocrystals was assumed to be equal to that of bulk gold.²¹ The observed deviation cannot be attributed to deficiencies of the effective medium approach because recent numerical studies reveal good agreement for the Maxwell–Garnett approximation of ϵ_{eff} compared to accurate finite element modeling for metallic inclusions with filling fractions within in the experimental range.²²

To isolate the effect of the nanocrystals on the optical properties of metallodielectric composites, the optical constants of thin films comprising PS-homopolymer/gold nanocrystal composites were studied using VASE. In spectroscopic ellipsometry, the ratio of the complex Fresnel reflection coefficients for transverse magnetic (TM, electric field vector in the plane of incidence) and transverse electric (TE, magnetic field vector in the plane of incidence) polarized light are measured as a function of wavelength and for varying angle of incidence. The ellipsometry results are expressed in terms of Ψ and Δ , which reflect amplitude ratio and phase, respectively, and which are related to the Fresnel reflection coefficients by

$$\tan(\psi) \exp(i\Delta) = \frac{\mathcal{R}_{\text{TM}}}{\mathcal{R}_{\text{TE}}} \quad (1)$$

where \mathcal{R}_{TM} and \mathcal{R}_{TE} are the complex Fresnel reflection coefficients for TM- and TE-polarized light, respectively. These coefficients contain the desired information about the material properties and physical dimensions and can be related to the optical constants of the film material by assuming a dispersion model describing the optical structure of the sample.²³ For our materials, we used a Gaussian-broadened polynomial superposition (GBPS) parametric dispersion model that has been described in detail elsewhere.²⁴ The GBPS model is fundamentally constructed by a superposition of piecewise continuous polynomials, which are numerically convolved with Gaussian oscillator line shapes. While this model does not directly capture the underlying physics of the material dielectric function, it has been shown to have a number of advantages when compared to other dispersion models: it is inductive, that is, it does not assume prior knowledge about the physical model of dispersion, and the resulting dielectric function is Kramers–Kronig-consistent.²⁵ The GBPS model has been successfully applied to a broad range of absorbing materials including crystalline and amorphous semiconductors, metals, and organics.²⁶ Figure 4 shows the experimental data for a PS/gold nanocrystal composite thin film with a metal particle filling fraction of $\phi = 0.06$, along with the respective fit to the dispersion model.²⁹

To relate the results to effective medium predictions, the morphology must justify the quasi-static approximation underlying EMT, which generally requires $R/\lambda \leq 0.02$ where R is a characteristic length scale of the dispersed component and λ is the wavelength of the electromagnetic wave.¹⁰ For nanocrystal/polymer composites, this amounts to the requirement of isolated particle morphology. Figure 5 shows an electron micrograph obtained by microsectioning a film of 100 μm thickness having a gold nanocrystal filling fraction $\phi = 0.06$. The micrograph reveals that aggregation is not significant upon embedding the

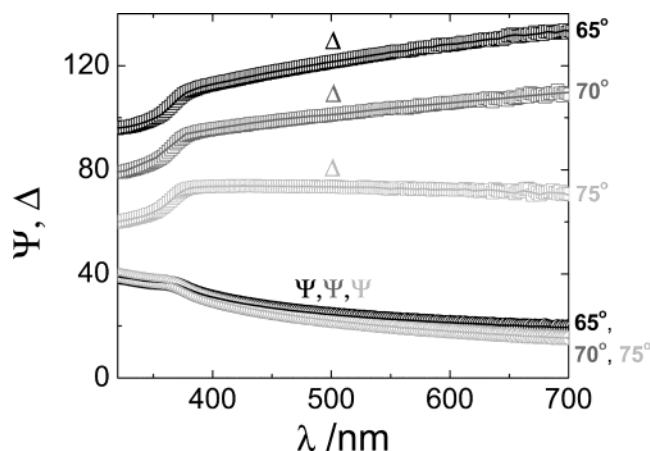


Figure 4. Plot of the amplitude ratio Ψ (\circ) and phase difference Δ (\square) of a PS/gold nanocrystal composite thin film with gold particle volume filling fraction $\phi = 0.06$ cast on a silicon substrate as determined by variable angle spectrometric ellipsometry (VASE) for angles of incidence $\theta = 65^\circ$, 70° , and 75° (dark, medium, and light gray, respectively), along with the respective fit using the GBPS dispersion model (solid lines).

PS-coated nanocrystals within a host PS homopolymer matrix, in accordance with the results obtained for the block copolymer nanocomposite. The isolated particle morphology of the embedded nanocrystals is also reflected in the absorption spectrum shown in the inset of Figure 5, which is virtually equal to absorption characteristics obtained from dilute solutions of the nanocrystals in toluene (not shown here) indicating the absence of connected particle aggregates.¹¹ For composites with arbitrary heterogeneities, an effective dielectric constant, ϵ_{eff} , can be derived that relates the average displacement in a composite material to the electric field via $\langle \mathbf{D}(x) \rangle = \epsilon_{\text{eff}} \langle \mathbf{E}(x) \rangle$ where $\langle \dots \rangle$

denotes the ensemble average. Assuming a random distribution of the heterogeneities, the following general expression for ϵ_{eff} is obtained using Green's function formalism¹⁰

$$\epsilon_{\text{eff}} = \epsilon_H + \frac{\langle (1 - (\epsilon_H - \epsilon_j)\Gamma_j)^{-1}(\epsilon_H - \epsilon_j) \rangle}{\langle (1 - (\epsilon_H - \epsilon_j)\Gamma_j)^{-1} \rangle} \quad (2)$$

Here, ϵ_H is a quantity that depends on the composite morphology and Γ_j is the depolarization tensor that depends on the geometry of the j th inclusion. It has been shown that, depending on the choice of ϵ_H , eq 1 recovers the Maxwell–Garnett, Lorentz–Lorenz, and Bruggemann approximations, which are three commonly used EMT models.¹⁰ The choice among these different approximations depends on the microstructure of the material. For composites consisting of discrete nanocrystals embedded in a polymer matrix, the Maxwell–Garnett (MG) model is the natural approximation that is obtained by setting ϵ_H in eq 2 to the matrix material. According to Maxwell–Garnett, ϵ_{eff} for the case of spherical nanocrystals is given by

$$\epsilon_{\text{eff}} = \epsilon_M \left(1 + 3 \frac{\phi x}{1 - \phi x} \right) \quad (3)$$

with $x = 1/3(\epsilon_P - \epsilon_M)/(\epsilon_M + 1/3(\epsilon_P - \epsilon_M))$; ϵ_P is the dielectric function of the nanocrystals, ϕ is the volume filling fraction of the nanocrystals, and $\epsilon_M = 2.53$ is the dielectric function of the matrix material (poly(styrene)), which is assumed to be constant within the frequency range under consideration.^{27,28} Note that the optical constants n_{eff} and k_{eff} , the real and imaginary part of the effective refractive index, are related to the effective dielectric function via $\epsilon_{\text{eff}} = (n_{\text{eff}}^2 - k_{\text{eff}}^2) + i(2n_{\text{eff}}k_{\text{eff}})$ with the imaginary unit i .

Shown in Figure 6 is the result obtained for n_{eff} and k_{eff} by VASE measurements of a PS/gold nanocrystal composite thin

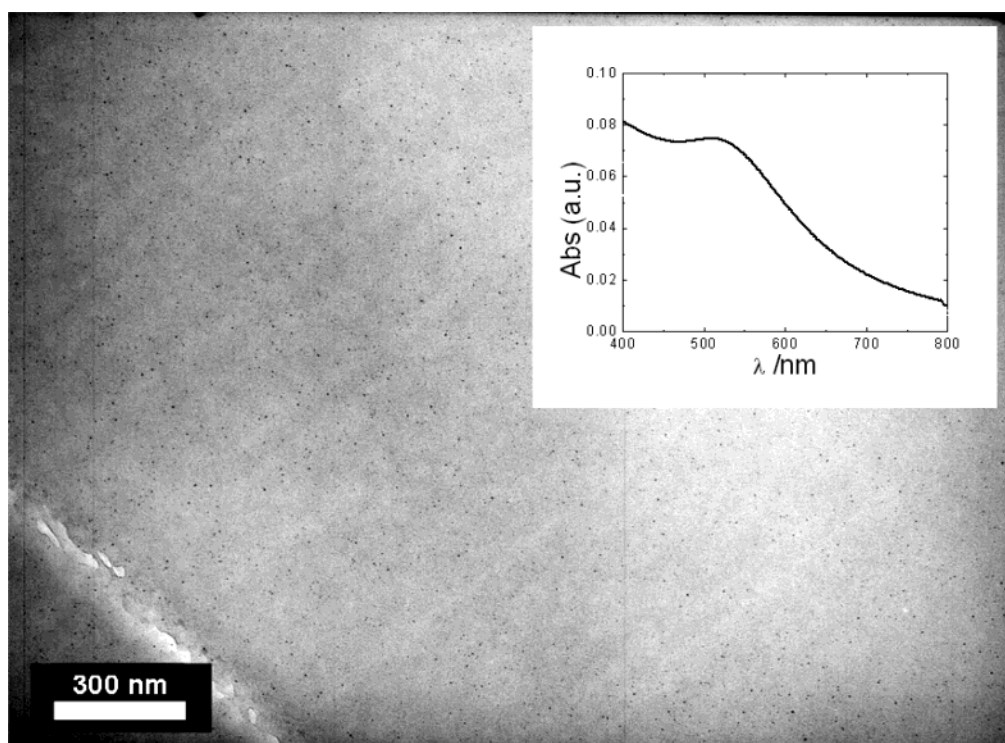


Figure 5. Transmission electron micrograph of a section of the poly(styrene)/gold nanocrystal composite film with particle filling fraction $\phi = 0.06$ revealing isolated nanocrystal morphology. Shown in the inset is the absorption spectrum of the respective film.

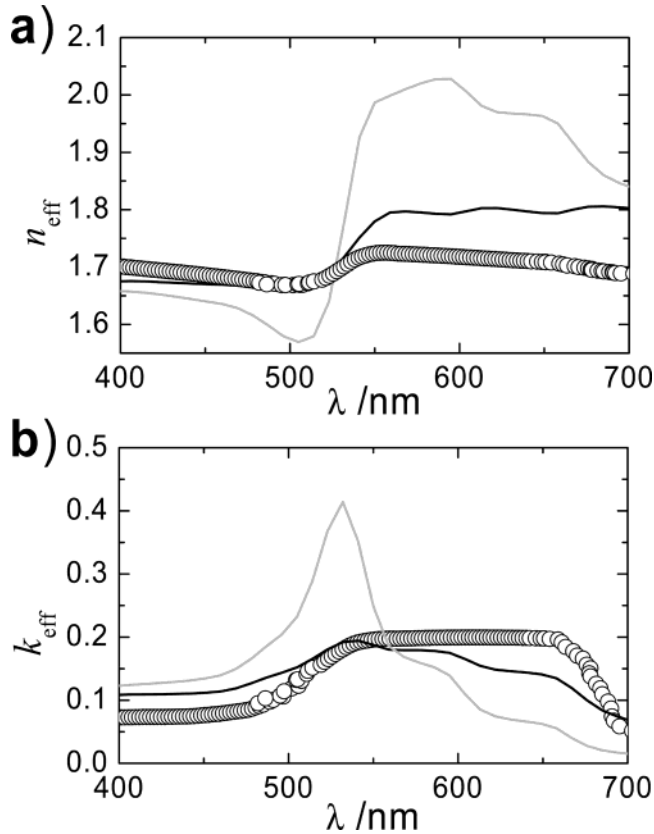


Figure 6. Comparison of the (a) real part, n_{eff} , and (b) imaginary part, k_{eff} , of the effective refractive index of poly(styrene)/gold nanocrystal composite ($\phi = 0.06$) determined by VASE assuming a GBPS dispersion model (O) and calculated using Maxwell-Garnett approximation (eq 3). Gray lines refer to calculation assuming bulk optical properties of gold,²¹ and black lines refer to calculation taking into account a mean free path corrected dielectric function as given in eq 4.

film having a particle filling fraction of $\phi = 0.06$, along with the calculated optical constants using MG theory.²⁹ Clearly MG theory does not account well for the measured optical constants if ϵ_p is assumed to be the bulk optical constant of gold as given by Palik,²¹ even though the composite's morphology indicates applicability of effective medium theory. The problem arises in the definition of the dielectric function of the dispersed metal component because it has been shown that a simple Drude-like model no longer applies when metals are confined to the nanometer lengthscale.^{8,30–32} Possible deviations of the dielectric function in confined systems from the bulk dielectric properties have been attributed to a limitation of the electron mean free path³³ and a damping of free electron oscillations induced by a discretization of the electronic structure.³⁴ Assuming normal fcc packing of the gold atoms within the particle, the average number of gold atoms per particle for a particle size of about $d_{\text{core}} = 3.2$ nm is about $N_{\text{Au}} = 59(\pi/6)d_{\text{core}}^3 \approx 10^3$ atoms. For free electron crystals of this size, the main effect on the dielectric function can be understood as a consequence of diffuse scattering of free electrons at the surface boundary.³¹ The result on the optical properties of the nanocrystals is an additional relaxation term in the Drude dielectric function such that $\Gamma(R) = \Gamma_{\infty} + \Delta\Gamma(R) = \nu_F/l_{\infty} + A\nu_F/R$, where Γ_{∞} is the bulk relaxation constant, $\nu_F = 1.4 \times 10^6$ m/s is the Fermi velocity, $l_{\infty} = 42$ nm is the bulk mean free path, and A is a theory-dependent constant that has been shown to be close to 0.6 for gold crystals of size $d_{\text{core}} \approx 3.2$ nm.³⁵ The dielectric function of the gold nanocrystals

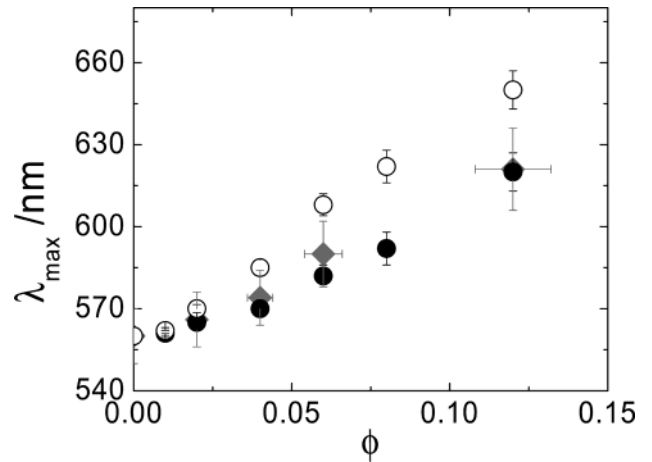


Figure 7. Comparison of the wavelength of maximum reflectivity, λ_{max} , at normal incidence as a function of particle filling fraction within the PS domain of a PS-PEP/gold nanocrystal composite as determined by subdomain reflectance measurements (◆) and calculated using the transfer matrix method and Maxwell-Garnett approximation. The O represents an effective medium assuming the optical properties of the nanocrystals to be equal to bulk optical properties; the ● represents a mean free path corrected dielectric function following eq 4.

is then given as

$$\epsilon_p(\omega, R) = \epsilon_{\text{bulk}}(\omega) + \omega_p^2 \left(\frac{1}{\omega^2 + \Gamma_{\infty}^2} - \frac{1}{\omega^2 + \Gamma(R)^2} \right) + i \frac{\omega_p^2}{\omega} \left(\frac{\Gamma(R)}{\omega^2 + \Gamma(R)^2} - \frac{\Gamma_{\infty}}{\omega^2 + \Gamma_{\infty}^2} \right) \quad (4)$$

where ϵ_{bulk} is the bulk dielectric constant of gold, ω is the radial frequency of the light, and $\omega_p = 1.35 \times 10^{16}$ rad/s is the plasma frequency of gold.^{36,37} As shown in Figure 6, taking into account the mean free path correction for the dielectric function of the metal particles, the agreement between the experimental values and effective medium calculation improves significantly even though effective medium theory overestimates the real part of the refractive index of our materials at longer wavelengths. Possible deviations might be attributed to the size distribution of the nanocrystals, as well as to the thiol ligands that are chemisorbed to the crystal surface and alter the electronic properties of surface gold atoms.³⁸ Because the number of available surface sites for a given amount of gold scales with the crystal diameter as d_{core}^{-1} , increasing deviations can be expected with decreasing crystal sizes.

Taking into consideration the results obtained for the optical properties of homo-PS/gold nanocrystal composites, the photonic properties of the block copolymer PS-PEP/gold nanocrystal composites can now be interpreted by representing each PS/nanocrystal layer in the stack as an effective layer taking into account confinement effects on the dielectric function of the nanocrystals. The calculation of the reflective properties of the composite material then reduces to calculating the reflectivity of a 1D multilayer stack via the transfer matrix method²⁰ using an effective dielectric function for the metal particle loaded PS domain as given by the MG formula. Figure 7 shows a comparison between the calculated and experimental values for the wavelength at peak reflectivity, λ_{max} . Note, that assuming a bulk dielectric function for the nanocrystalline gold results in an overestimation of the observed red shift of λ_{max} upon particle sequestration by about $\Delta\lambda_{\text{max}}/\lambda_{\text{max}} = 45\%$ at $\phi = 0.12$, indicating a profound influence of crystal size-specific contributions to

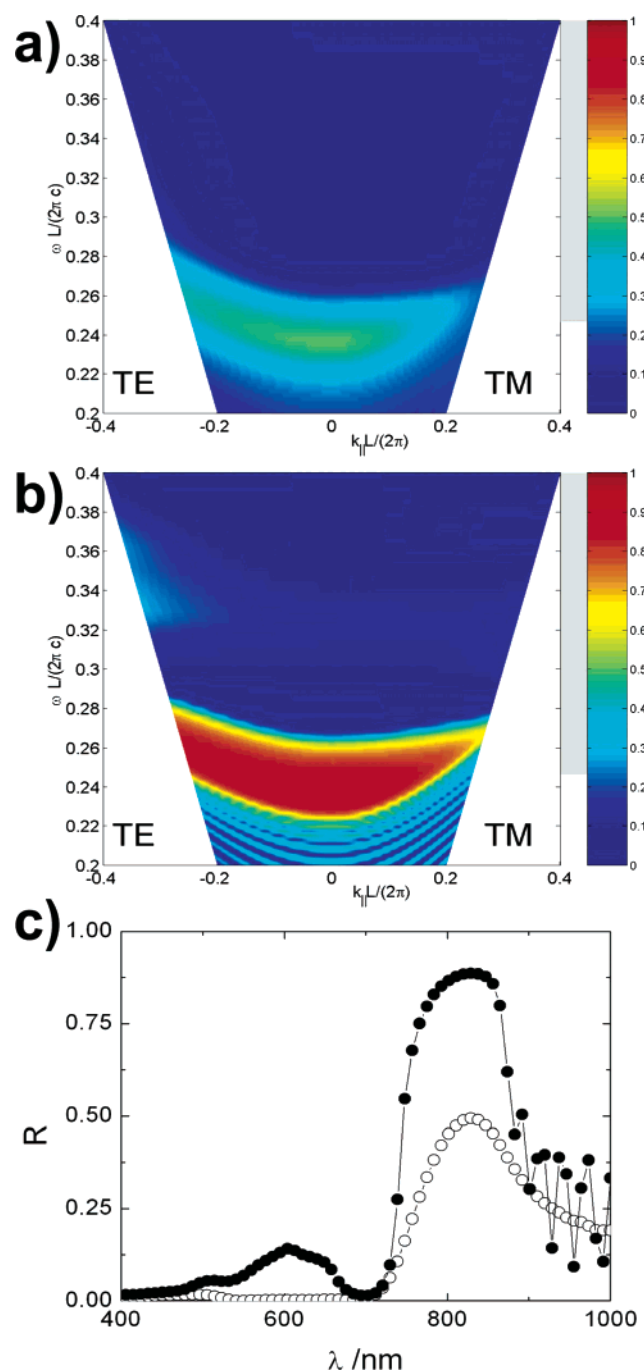


Figure 8. Calculated frequency dependence of reflectivity for TE and TM polarization for a PS–PEP stack with a gold crystal filling fraction of $\phi = 0.2$ in the PS domain. The simulation in panel a assumes the corrected dielectric function of the nanocrystals for a particle diameter $d_{\text{core}} = 3.2$ nm; that in panel b assumes a particle diameter $d_{\text{core}} = 42$ nm $= l_{\infty}$. The calculation refers to a periodicity of 30 double layers, $d_{\text{PS}} = 100$ nm, $n_{\text{PS}} = 1.59$, $d_{\text{PEP}} = 80$ nm, and $n_{\text{PEP}} = 1.49$; the ambient medium is air; $L = d_{\text{PS}} + d_{\text{PEP}}$ is the lamellar thickness, ω denotes the radial frequency, c is the vacuum speed of light, and k_{\parallel} is the parallel component of the wavevector with respect to the layer orientation. Panel c shows the wavelength-dependent reflectivity obtained from panels a and b for normal incidence ($k_{\parallel} = 0$): (○) $d_{\text{core}} = 3.2$ nm; (●) $d_{\text{core}} = 42$ nm. The gray bars in panels a and b indicate the visible frequency range ($\lambda = 400$ – 700 nm). For all calculations, the refractive index of the polymer components is assumed to be wavelength-independent.

the optical response of the nanocomposite.³⁹ This demonstrates that the effect of spatial confinement on the optical properties of nanocrystals has to be considered when designing composite materials for photonic applications.

The effect of crystal diameter on the optical properties of the periodic composite can be demonstrated by comparing the reflective properties that are expected for the layered composite structures assuming a particle size of $d_{\text{core}} = 3.2$ and $d_{\text{core}} = l_{\infty} = 42$ nm, respectively, where for the latter particle size the optical constants were found to be close to bulk values.³⁵ Following the conventions for photonic band structure representations, we display the reflection spectra in terms of the reflectivity at reduced frequency $\omega L/(2\pi c)$, c denoting the vacuum velocity of light, and reduced parallel wavevector $k_{\parallel}L/(2\pi)$ with $k_{\parallel} = (2\pi/\lambda)\sin\theta$, where θ is the angle of incidence (measured with respect to the layer normal). Figure 8a,b shows the calculated reflectivity spectra for TE- and TM-polarized incident light of a composite multilayer stack identical to our system, assuming a gold volume filling fraction within the PS domain of $\phi = 0.2$ and assuming a particle diameter $d_{\text{core}} = 3.2$ nm and $d_{\text{core}} = 42$ nm, respectively.⁴⁰ The comparison of the reflection spectra reveals that neglecting the confinement effect on the crystal dielectric function results in substantial overestimation of the maximum reflectivity and the wavelength of maximum reflection, as well as an inaccurate prediction of the reflection characteristics of TE- and TM-polarized light for oblique angles of incidence. The gap width to center ratio, $\Delta\lambda_{\text{max}}/\lambda_{\text{max}}$ is overestimated by 20% when bulk optical constants are assumed as demonstrated in Figure 8c for the case of normal incidence.

Conclusions

Preferential sequestering of polymer-grafted gold nanocrystals into self-assembled diblock copolymers provides a means to obtain nanocomposite materials for photonic applications that capitalize on both the optical properties of the periodic microstructured template material and the optical properties of the sequestered nanocrystals. Realistic modeling and prediction of the photonic characteristics of periodic composite materials *must* account for size-, and therefore sample-, specific effects that alter the optical properties of the constituent materials and hence influence the optical response of the composite. The latter issue results in the necessity to develop synthetic methodologies that allow for the preparation of microstructured composites with well-defined particle size and shape distribution, as well as a regular morphology of the dispersed component within the composite material. Confinement effects on the dielectric function of free electron nanocrystals result in a lower rejection level for incident light at visible wavelengths than is predicted by assuming bulk optical properties. Within the free electron model described above and assuming isolated nanocrystal morphology, the electron mean free path provides an important length scale governing confinement effects on the photonic properties of composite materials. The results suggest that for engineering polymer-based metallodielectric materials with high rejection levels for incident light, particle sizes on the order of the electron's mean free path should be used provided their size is below the scattering limit for the range of wavelengths of interest.

Acknowledgment. This research was supported by, or supported in part by, the U.S. Army through the Institute for Soldier Nanotechnologies, under Contract DAAD-19-02-D0002 with the U.S. Army Research Office, as well as the Alexander von Humboldt foundation (Feodor-Lynen program). The support of Prof. K. Gleason and Dr. Quingo Wu for performing the VASE experiments is gratefully acknowledged.

Supporting Information Available: Comparison of the respective film thickness of PS/Au-nanocrystal thin films as

determined by VASE and profilometry; absorption and scattering cross section of gold nanocrystals ($d = 42$ nm) calculated using Mie theory. This material is available free of charge via the Internet at <http://pubs.acs.org>.

References and Notes

- (1) Yablonovitch, E. *Phys. Rev. Lett.* **1987**, *58*, 2059–2062.
- (2) John, S. *Phys. Rev. Lett.* **1987**, *58*, 2486–2489.
- (3) Fink, J.; Winn, J. N.; Fan, S.; Chen, C.; Michel, J.; Joannopoulos, J. D.; Thomas, E. L. *Science* **1998**, *282*, 1679–1682.
- (4) Berger, V. *Curr. Opin. Solid State Mater. Sci.* **1999**, *4*, 209–216.
- (5) Edrington, A. C.; Urbas, A. M.; DeRege, P.; Chen, X. C.; Swager, T. M.; Hadjichristidis, N.; Xendiou, M.; Fetters, L. J.; Joannopoulos, J. D.; Fink, Y.; Thomas, E. L. *Adv. Mater.* **2001**, *13*, 421–424.
- (6) Urbas, A. M.; Maldovan, M.; Carter, C.; Yufa, N.; Thomas, E. L. *Adv. Mater.* **2002**, *14*, 1853–1856.
- (7) Richards, H. B. *Eur. J. Inorg. Chem.* **2001**, 2455–2480.
- (8) El-Sayed, M. A. *Acc. Chem. Res.* **2001**, *34*, 257–264.
- (9) Bockstaller, M. R.; Kolb, R.; Thomas, E. L. *Adv. Mater.* **2001**, *13*, 1783–1786.
- (10) Choy, T. C. *Effective Medium Theory*; Oxford University Press: Oxford, U.K., 1999.
- (11) Simon, R.; Ulrich, P. *Colloid Polym. Sci.* **1999**, *277*, 2–14.
- (12) Smith, D. D.; Snow, L. A.; Sibille, L.; Ignont, E. *J. Non-Cryst. Solids* **2001**, *285*, 256–263.
- (13) Brust, M.; Bethell, D.; Schiffrin, D. J.; Whyman, R. J. *Chem. Soc., Chem. Commun.* **1994**, 801–802.
- (14) Kiely, C. J.; Fink, J.; Brust, M.; Bethell, D.; Schiffrin, D. J. *Nature* **1998**, *396*, 444–446.
- (15) Antonietti, M.; Forster, S.; Hartmann, J.; Oestreich, S.; Wenz, E. *Nachr. Chem. Tech. Lab.* **1996**, *44*, 579.
- (16) Qu, S.; Du, C.; Wang, Y.; Gao, Y.; Liu, S.; Liu, Y.; Zhu, D. *Opt. Commun.* **2001**, *196*, 317–323.
- (17) Bockstaller, M. R.; Lapetnikov, Y.; Margel, S.; Thomas, E. L. *J. Am. Chem. Soc.* **2003**, *125*, 5276–5277.
- (18) Cohen, R. E. *Curr. Opin. Solid State Mater. Sci.* **1999**, *4*, 587–590.
- (19) Cohen, R. E. In *Polymeric Materials*; Salamone, J. C., Ed.; CRC Press: Boca Raton, FL, 1996; Vol. 6, pp 4143–4149.
- (20) Born, M.; Wolf, M. *Theory of optics*; Cambridge University Press: London, 2000.
- (21) Palik, E. D. *Handbook of Optical Constants of Solids*; Academic Press: San Diego, CA, 1998; Vol. 1.
- (22) Maldovan, M.; Bockstaller, M. R.; Thomas, E. L.; Carter, C. *Appl. Phys. B* **2003**, *76*, 877–884.
- (23) Woolham, J. A.; Bungay, C. L.; Synowicki, R. A.; Tiwald, T. E.; Thompson, T. W. In *Characterization and Metrology for ULSI Technology, 2000: International Conference, Gaithersburg, Maryland, 26–29 June 2000*; Seiler, D. G., Shaffner, T. J., McDonald, R., Bullis, W. M., Smith P. J., Secula, E. M., Eds.; American Institute of Physics: Melville, NY, 2001; Vol. CP550, pp 511–518.
- (24) Herzinger, C. M.; Johs, B. D. U.S. Patent 5,796,983, August 18, 1998.
- (25) Johs, B.; Herzinger, C. M.; Hilfiker, J.; Synowicki, R.; Bungay, C. L. In *Optical Metrology*; Society of Photo-Optical Instrumentation Engineers: Denver, CO, 1999; Vol. CR72, pp 29–58.
- (26) Jellison, G. E. *Opt. Mater.* **1992**, *1*, 41.
- (27) Garnett, J. C. M. *Philos. Trans. R. Soc.* **1904**, *203*, 385–420.
- (28) Garnett, J. C. M. *Philos. Trans. R. Soc.* **1906**, *205*, 237.
- (29) To test the reliability of the ellipsometric results, we independently determined the film thickness of all samples by profilometry, and the values obtained with both methods were found to agree within the range of experimental error (see Supporting Information, Figure S1).
- (30) Whetten, R. L.; Khoury, J. T.; Alvarez, M. M.; Murthy, S.; Vezmar, I.; Wang, Z. L.; Stephens, P. W.; Cleveland, C. L.; Luedtke, W. D.; Landman, U. *Adv. Mater.* **1996**, *8*, 428–431.
- (31) Alvarez, M. M.; Khoury, T. J.; Schaaff, G. T.; Shafigullin, M. N.; Vezmar, I.; Whetten, R. L. *J. Phys. Chem. B* **1997**, *101*, 3706–3712.
- (32) Bigioni, T. P.; Whetten, R. L.; Dag, O. *J. Phys. Chem. B* **2000**, *104*, 6983–6986.
- (33) Fragstein, U.; Kreibig, U. *Z. Phys.* **1969**, *224*, 307–323.
- (34) Kawabata, A.; Kubo, R. *J. Phys. Soc. Jpn.* **1966**, *21*, 1765.
- (35) Quinten, M. *Z. Phys. B* **1996**, *101*, 211–217.
- (36) Kreibig, U. *Z. Phys.* **1970**, *234*, 307–318.
- (37) Vollmer, U.; Kreibig, U. *Optical Properties of Metal Clusters*; Springer-Verlag: Berlin, Heidelberg, New York, 1995; Vol. 1.
- (38) Fenter, P.; Eberhardt, A.; Eisenberger, P. *Science* **1994**, *266*, 1216–1218.
- (39) In calculating the reflectivity R of the layered nanocomposite, one needs to take into account that the layer spacings of the respective block copolymer domains change upon particle sequestering. The effect of particle incorporation on the morphology of lamellar block copolymers has been discussed theoretically (see: Hamdoun, B.; Ausserre, D.; Cabuil, V.; Joly, S. *J. Phys. 2 France* **1996**, *6*, 503–510). Assuming a symmetric lamellar morphology of the PS–PEP block copolymer and a homogeneous distribution of the nanocrystals within the PS host domain, the change in layer spacing of the respective domains upon particle deposition can be shown to be $d_{PS} = d_{PS}^0(1 + 4\phi^*/3)$, $d_{PEP} = d_{PEP}^0(1 - 2\phi^*/3)$, and hence, $L = L_0(1 + \phi^*/3)$ with $L = d_{PS} + d_{PEP}$. Here, $\phi^* = \phi(1 + ((d_{core}/2 + r_g)^3 - (d_{core}/2)^3)/(d_{core}/2)^3)$ is the volume contribution of the polymer-coated nanoparticles with metal volume filling fraction ϕ and assuming the grafted polymer layer around each particle to be an impenetrable shell of thickness r_g ; d_{core} denotes the particle core diameter, d_X^0 represents the layer thickness of the X-domain in the neat block copolymer, and L_0 represents the respective lamellar thickness.
- (40) Calculation of the scattering and extinction cross sections of individual gold nanocrystals embedded in PS matrix using Mie theory reveals that the quasi-static approximation remains valid for the case of particle sizes of $d_{core} = 42$ nm (see Supporting Information, Figure S2).